Extensive carbon isotopic heterogeneity among methane seep microbiota

Christopher H. House,[1]* Victoria J. Orphan,[2]*
Kendra A. Turk,[2] Burt Thomas,[1]
Annelie Pernthaler,[2]† Jennifer M. Vrentas,[1] and
Samantha B. Joye[3]

[1]*Department of Geosciences and Penn State
Astrobiology Research Center, The Pennsylvania State
University, 220 Deike Building, University Park, PA
16802, USA.*
[2]*Division of Geological and Planetary Sciences,
California Institute of Technology, Pasadena, CA 91125,
USA.*
[3]*Department of Marine Sciences, University of Georgia,
Athens, GA 30602, USA.*

Summary

To assess and study the heterogeneity of $\delta^{13}C$ values for seep microorganisms of the Eel River Basin, we studied two principally different sample sets: sediments from push cores and artificial surfaces colonized over a 14 month *in situ* incubation. In a single sediment core, the $\delta^{13}C$ compositions of methane seep-associated microorganisms were measured and the relative activity of several metabolisms was determined using radiotracers. We observed a large range of archaeal $\delta^{13}C$ values (> 50‰) in this microbial community. The $\delta^{13}C$ of ANME-1 rods ranged from –24‰ to –87‰. The $\delta^{13}C$ of ANME-2 sarcina ranged from –18‰ to –75‰. Initial measurements of shell aggregates were as heavy as –19.5‰ with none observed to be lighter than –57‰. Subsequent measurements on shell aggregates trended lighter reaching values as ^{13}C-depleted as –73‰. The observed isotopic trends found for mixed aggregates were similar to those found for shell aggregates in that the initial measurements were often enriched and the subsequent analyses were more ^{13}C-depleted (with values as light as –56‰). The isotopic heterogeneity and trends observed within taxonomic groups suggest that ANME-1 and ANME-2 sarcina are capable of both methanogenesis and methanotrophy. *In situ* microbial growth was investigated by incubating a series of slides and silicon (Si) wafers for 14 months in seep sediment. The experiment showed ubiquitous growth of bacterial filaments (mean $\delta^{13}C = -38 \pm 3$‰), suggesting that this bacterial morphotype was capable of rapid colonization and growth.

Introduction

The anaerobic oxidation of methane (AOM) is the microbial process by which marine methane is oxidized to dissolved inorganic carbon (DIC) while sulfate is reduced to sulfide (Valentine, 2002 and references therein). AOM's resultant porewater geochemical profiles were first observed in coastal marine sediments (Barnes and Goldberg, 1976; Reeburgh, 1976). The microbial communities mediating AOM oxidize an estimated 300 Tg of CH_4 a year (Hinrichs and Boetius, 2002), minimizing CH_4 release from marine environments as marine sediment fluxes account for only 2% of the global atmospheric CH_4 source (Reeburgh, 1996). Despite the importance of AOM to the global methane and carbon cycles the microbes responsible for AOM have not been successfully grown in pure culture. This fact makes culture-independent techniques of the utmost importance.

There are at least three distinct groups of *Archaea* (ANME-1, ANME-2 and ANME-3) associated with AOM (Knittel *et al.*, 2005), and these groups show phylogenetic affinity with cultured methanogen species (Hinrichs *et al.*, 1999; Orphan *et al.*, 2001a; Teske *et al.*, 2002). Fluorescence *in situ* hybridization (FISH) imaging shows that hese groups often exist in close physical relationships in spherical consortia clusters with archaeal cores and bacterial shells (Boetius *et al.*, 2000). In nature, ANME are commonly paired with δ-proteobacterial partners that have high genetic similarity to known sulfate-reducing bacteria (SRB) (Orphan *et al.*, 2001a; Niemann *et al.*, 2006; Leloup *et al.*, 2007; Pernthaler *et al.*, 2008).

Stable carbon isotope analyses of specific lipid biomarkers document the assimilation of CH_4 carbon, first by an archaeal methanotroph then by a bacterial sulfate reducer (Hinrichs *et al.*, 1999; 2000; Pancost *et al.*, 2000; Michaelis *et al.*, 2002). Isotopic measurements of individual cells confirm CH_4 oxidation by the consortia, and also suggest

that single archaeal cells may maintain viable AOM activity (Orphan *et al.*, 2002). AOM activity is strongly correlated with the abundance of certain archaeal species closely related to methanogenic lineages. This relationship suggests that these microorganisms may have reversible metabolisms, allowing an individual species to alternate between methanotrophic and methanogenic metabolic modes (Hoehler, 1994; Orcutt *et al.*, 2005).

Diverse molecular and isotopic tools have opened up the study of AOM communities, although several important points of inquiry remain. First, the mechanism of electron transfer between methanotrophic archaea and SRB consorts is still unknown (Nauhaus *et al.*, 2002; Moran, 2008). Second, it is unclear which, if any, of the methanotrophic archaea can reverse their metabolism and grow methanogenically. Third, the extent to which AOM communities decouple methanotrophy from sulfate reduction is unclear. Fourth, the degree to which methane oxidation alters the carbon isotopic composition of a wide range of methane seep-associated microorganisms remains largely undocumented.

To assess and study the heterogeneity of δ^{13}C values for microorganisms living in methane vents of the Eel River Basin, we studied two principally different sample sets: sediments from push cores and silicon wafer surfaces colonized over a 14 month *in situ* incubation. Here, we used FISH and secondary ion mass spectrometry (SIMS) (Orphan *et al.*, 2001b) to reveal the carbon isotopic heterogeneity of seep-associated archaeal and bacterial cells at four depths in the sediment. On the same sediment core, we also conducted radiotracer experiments ($^{14}CH_4$, $^{35}SO_4^{2-}$, $H^{14}CO_3^-$ and $^{14}CH_3^{14}COO^-$) to measure relative rates of methane oxidation, sulfate reduction and methanogenesis (Orcutt *et al.*, 2005). The results were used to address the potential relationships between methanotrophy and methanogenesis and the extent of metabolism coupling by seep-associated microorganisms. To examine *in situ* microbial growth and corresponding δ^{13}C values of new microbial biomass, a 14 month incubation experiment within seep sediment was conducted using a 'peeper' device equipped with colonization surfaces (glass slides and silicon wafers). After recovery, the morphology and broad identification of microorganisms adhered to the incubated slides were determined using scanning electron microscopy (SEM) and FISH and the carbon isotopic compositions of the attached microorganisms and related biofilm were subsequently analysed by SIMS (House *et al.*, 2000).

Results and discussion

Push-core sediments

The first part of our work reported here is focused on a pair of push cores taken from the Northern Ridge of the Eel River Basin methane seeps off the coast of California with PC59 providing a porewater geochemical profile and PC55 used to pair radiotracer measurements of metabolic rates with carbon isotopic analyses of FISH-identified cells. PC59 shows fairly typical profiles for porewater geochemistry within a methane vent (Fig. 1). As expected, sulfate concentrations decrease from seawater values with increasing depth due to microbial sulfate reduction. Both DIC and sulfide concentrations
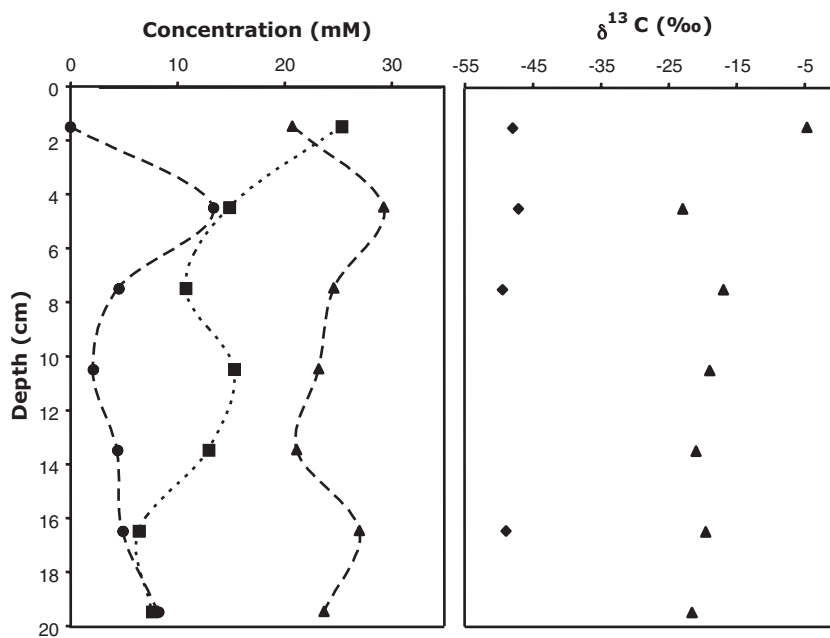

Fig. 1. A. Porewater geochemistry observed in PC59: (●) sulfide concentrations, (■) sulfate concentrations and (▲) dissolved inorganic carbon.
B. Porewater δ^{13}C values observed in PC59: (◆) methane and (▲) dissolved inorganic carbon.
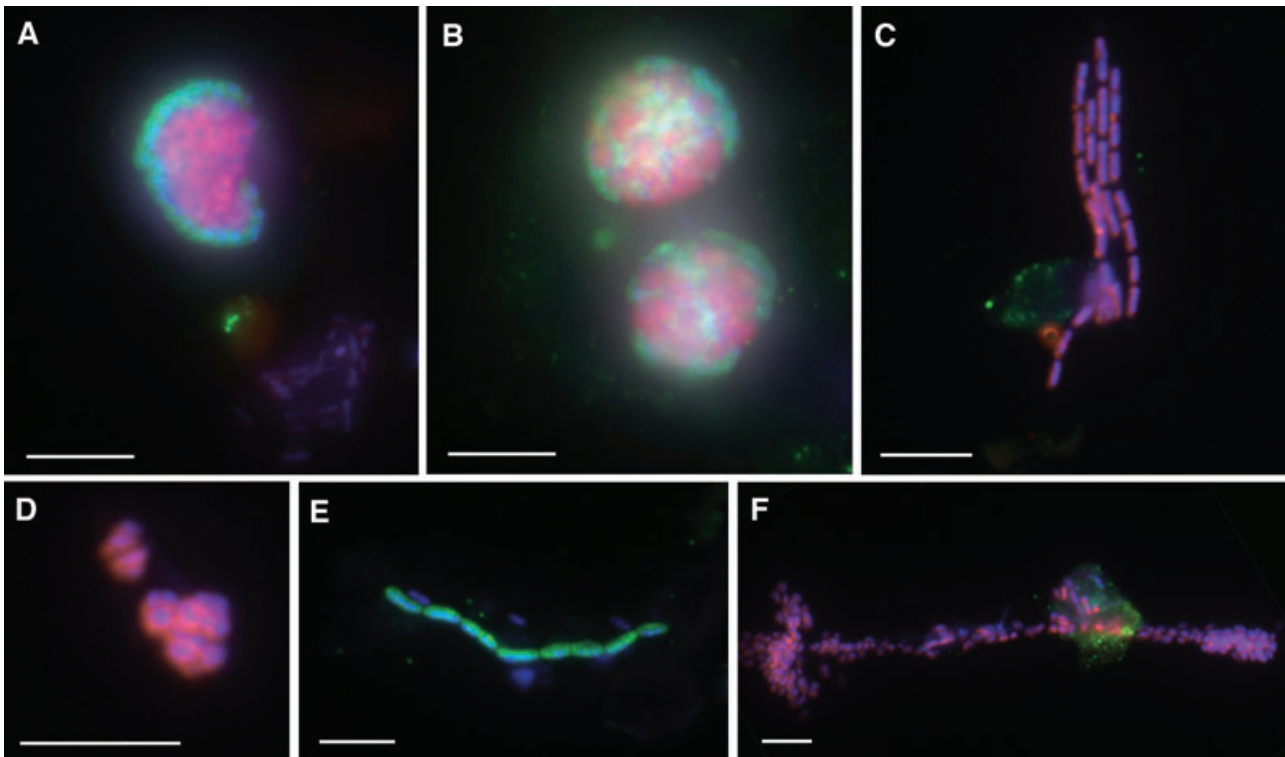
Fig. 2. PC55 Seep microbiota observed and studied on glass slides with FISH-SIMS: (A) shell aggregate (FC_sp25), (B) mixed aggregate (FD_sp26), (C) ANME-1 rods (FB_sp27A). (D) Archaeal sarcina (FD_sp28), (E) bacterial filaments (FC_sp26) and (F) archaeal sarcina in a 'string of pearls' morphology (FB_sp19).

are elevated at depth resulting from both sulfate reduction and AOM. Methane concentrations were consistent over depth (~1785 μM) and had an observed average $\delta^{13}C$-CH_4 of −48.4‰ (see Orphan *et al.*, 2004 for geological and geochemical context). In contrast, the observed $\delta^{13}C$ of the DIC in surface sediments was −4.5‰, it decreased to an average of −20.2‰ at depth. These carbon pools provide the basis for the interpretation of the $\delta^{13}C$ signatures of the microbial community inhabiting nearby PC55. Figure 2 shows a selection of diverse microbial associations observed with FISH from PC55 samples. As has commonly been documented in cold seep settings (Boetius *et al.*, 2000; Orphan *et al.*, 2001a; 2002; Knittel *et al.*, 2005; Orcutt *et al.*, 2005), we observed shell aggregates with ANME-2 archaeal cores and bacterial shells (Fig. 2A), mixed aggregates that contain heterogeneous distribution of ANME-2 and SRB cells (Fig. 2B), ANME-1 rods and filaments (Fig. 2C), archaeal ANME-2 sarcina observed independent of bacteria (Fig. 2D), and bacterial rods and filaments (Fig. 2E). In addition, we observed several cases of long drawn-out clusters of archaeal sarcina, resembling a 'string of pearls' morphology (Fig. 2F).

The $\delta^{13}C$ values from the various cell types are listed in Table S1 and shown as a function of sediment depth in Fig. 3A. For each analysis, the initial observed value is

shown as a large point and subsequent analyses are represented as small points. This was done because as the ion microprobe sputters into and then through cell clusters, the isotopic results often show dramatic trends, such as a significantly more ^{13}C-depleted archaeal core for shell aggregates. Overall, the $\delta^{13}C$ of ANME-1 rods ranged from −24‰ to −87‰. The $\delta^{13}C$ of ANME-2 sarcina ranged from −18‰ to −75‰. As previously observed, the $\delta^{13}C$ of shell aggregates trended towards more ^{13}C-depleted values as the analysis proceeded through the bacterial shell and into the archaeal core (Orphan *et al.*, 2001b; 2008). Initial measurements of shell aggregates, which represent the bacterial shell and any surrounding extracellular polymeric substance, were as heavy as −19.5‰ with none observed to be lighter than −57‰. Subsequent measurements on shell aggregates trended lighter reaching values as ^{13}C-depleted as −73‰. The isotopic trends observed in mixed aggregates were similar to those observed in shell aggregates, except that they did not reach such depleted $\delta^{13}C$ values. Initial measurements on shell aggregates were as enriched as −24‰, and subsequent analyses (sputtering into the aggregate) were as depleted as −56‰. These results suggest that, in the case of the mixed aggregate, the initial isotopic measurement is largely sampling bacterial extracellular polymeric substance, and then subsequent mea-
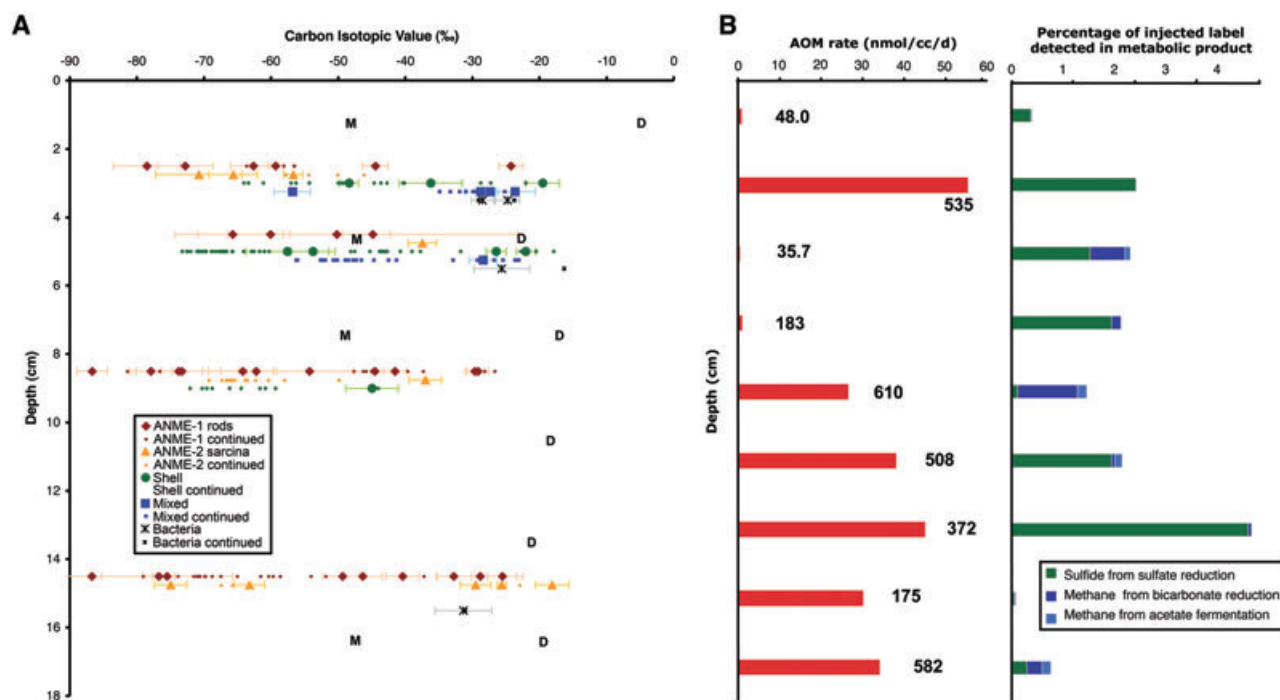
Fig. 3. A. The $\delta^{13}C$ compositions of various taxa observed as a function of depth in PC55. Large points show the initial data, with subsequent cycles shown as small points. Also shown are the isotopic compositions of porewater methane (M) and DIC (D) from various depths of PC59. Because these data are from a separate core, they should be considered only as an approximate guide for context.
B. Observed rates of methane oxidation. The numbers shown by each bar is the measured porewater methane concentration (μM).
C. Observed relative rates of sulfate reduction, CO_2-reductive methanogenesis, and acetoclastic methanogenesis.

surements show an intermediate isotopic value as the beam samples a mixture of archaeal and bacterial cellular material. In PC55, bacterial filaments independent of archaeal cells had $\delta^{13}C$ values around −28‰.

Several clear trends are apparent from these data. First, shell and mixed aggregates were considerably more common in the shallower depths (0–6 cm), and were absent from the deepest horizon studied (14–16 cm). Second, ANME-1 rods and ANME-2 sarcina were found at all depths investigated, but the prevalence of ANME-1 increased at depth, making it the most commonly observed group in the 14–16 cm sample. Third, at almost all depths, the most ^{13}C-depleted cells were ANME-1. Fourth, overall, there is a very large range of carbon isotopic values in this microbial community with the observed values typically ranging from roughly the isotopic value found for porewater DIC to > 30‰ lighter than the value for porewater methane. Finally, we clearly observe large isotopic heterogeneity (tens of ‰) within both the ANME-1 and ANME-2 populations.

Overprinting in an integrated seepage system could contribute to the isotopic heterogeneity of seep microorganisms. Gases and liquids found in the sediments of the Eel River Basin are known to have a range of hydrocarbons (Kvenvolden and Field, 1981) allowing for some shift

in the mix of carbon sources over time. In particular, such overprinting might especially influence the $\delta^{13}C$ composition of bacteria present alone or as members of consortia. There appears to be significant metabolic and phylogenetic diversity in the SRB involved in AOM. For example, Pernthaler and colleagues (2008) found that ANME can be physically coupled to at least three different bacterial lineages.

It is unlikely that overprinting is principle explanation, however, for the very large isotopic heterogeneity observed for seep archaea because methane is the dominant hydrocarbon in Eel River Basin seepage. The remarkable isotopic heterogeneity within these taxonomic groups probably indicates that ANME-1 and at least some archaeal sarcina are capable of both methanogenesis and methanotrophy. Under this interpretation, acetoclastic methanogenic growth would account for the isotopically enriched cells, while methanotrophy provides the most ^{13}C-depleted cells. In acetoclastic merthanogenesis, cell biomass would be derived from available acetate rather than the strongly ^{13}C-depleted methane. Also, it is known that acetoclastic methanogenesis produces relatively small isotopic fractionations (Krzycki *et al.*, 1987). These results could either demonstrate that submembers of each group are performing these differ-

ent metabolisms separately, or that some archaea switch between methanogenesis and methanotrophy. The later interpretation supports the 'reverse methanogenesis' hypothesis for the biochemistry of AOM (Hoehler, 1994; Hallam *et al.*, 2004). While genomic evidence supports the potential for methanogenic growth in addition to methanotrophy (Hallam *et al.*, 2004), our isotopic study alone cannot rule out the possibility that these archaeal groups are, at times, heterotrophic rather than acetoclastic. In this alternative, methanotrophic growth still provides the most ^{13}C-depleted cells, while heterotrophy results in less ^{13}C-depletion. Past work using labelled tracer has documented the transfer of comparable amounts of both CO_2 and methane into ANME biomass making it clear that these cells accumulate carbon from more than one source (Wegener *et al.*, 2008). Additional experiments are necessary to directly test the ability of these ANME archaeal groups to assimilate more complex sources of carbon.

The variability of metabolic rates with depth is also supportive of reverse methanogenesis (Fig. 3B). The rate of AOM is highest in the 2–4 cm horizon, but otherwise quite low from the surface down to 8 cm. Below 8 cm, the rate of AOM climbs and is constant at around 40 nmol methane per cc per day. Importantly, despite the similarities in microbial populations between the 2–4 cm sample and the 4–6 cm sample, these two horizons show the highest and lowest AOM rates. The contrast between these two samples is further highlighted by the lack of methanogenesis at 2–4 cm and relatively high methanogenesis at 4–6 cm. The most noticeable difference in the FISH-SIMS results from these two horizons is the absence of highly ^{13}C-depleted ANME-1 or sarcina cells from the AOM poor 4–6 cm horizon (Fig. 3A). However, depleted values are observed within shell aggregates found at both horizons with similar isotopic ranges (Fig. 3A). The data set is too limited to have high confidence in the lack of highly ^{13}C-depleted ANME-1 or sarcina at 4–6 cm, but the observation is consistent with the presence of methanogenic archaea with carbon isotopic compositions that migrate towards heavier values during methanogenic episodes.

Colonized artificial surfaces

The second part of this environmental study consisted of a year-long *in situ* incubation experiment that placed glass slides and silicon wafers into a methane seep for 14 months. Upon inspection with phase-contrast light microscopy (for glass slides) and reflected light microscopy (for the silicon wafers), numerous filaments were found on all slides and wafers that were submerged below the sediment water interface. The morphology of the extensive filamentous growth was unchanged from

slide to slide, suggesting that the same microbial group grew in all samples. As might be expected, the growth observed in slides behind 12 μm filters was more extensive than that found for slides behind 0.2 μm filters. However, significantly more microbial colonization was found on samples behind the 0.2 μm filters than was initially anticipated.

The density of cells found on the samples protected by a 0.2 μm filter was ideal for a SIMS study with numerous cells separated from each other. The third depth interval of the 0.2 μm series was chosen for further study (corresponding to a sediment depth of ~8 cm). The glass slide was used for FISH to identify the taxonomic affinity of the ubiquitous filaments, and the silicon wafer was used for SEM followed by SIMS. The results (Fig. 4) indicate that the ubiquitous filaments were bacterial (Fig. 4A) and they did not appreciably incorporate ^{13}C-depleted carbon from the methane seep (Fig. 4B–D), with a δ^{13}C weighted mean of −38 ± 3‰. The lack of isotopic evidence of methanotrophy found in this experiment was disappointing, as it provided little information for interpreting seep microbiology. If these filaments were sulfide oxidizers, the presence of the filaments on slides and wafers of all depths might indicate that the disruption of the mat caused by the insertion of the peeper provided a conduit for seawater nitrate to some depth. In any case, the ubiquity of the observed filaments (even behind a 0.2 μm filter) suggests that this bacterial morphotype was capable of rapid colonization and growth, probably more rapid than ANMEs. With this interpretation, one can envision that the observed *in situ* growth represents only the initial stage of seep community reformation on the slides and wafers. It is likely that additional seep microbiota are present on the recovered slides, although at lower cell densities.

Conclusions

In summary, from this new work, we conclude that extensive carbon isotopic heterogeneity exists within archaeal methane seep taxa. Our work also shows that bacteria found alone in the seep sediment or grown *in situ* on silicon or glass placed into the seep sediment do not show the strong isotopic signature of methanotrophy. Together these results confirm the primary role that ANME-1 and ANME-2 have in the AOM. The δ^{13}C values for cells observed in the seep sediment also, taken together with our metabolic rate data, suggest that some of the archaeal phylotypes also can perform methanogenesis. In particular, the ANME-1 cells are found throughout the sediment core and often have isotopic compositions that span 50‰. Such remarkable isotopic heterogeneity within populations and on such small
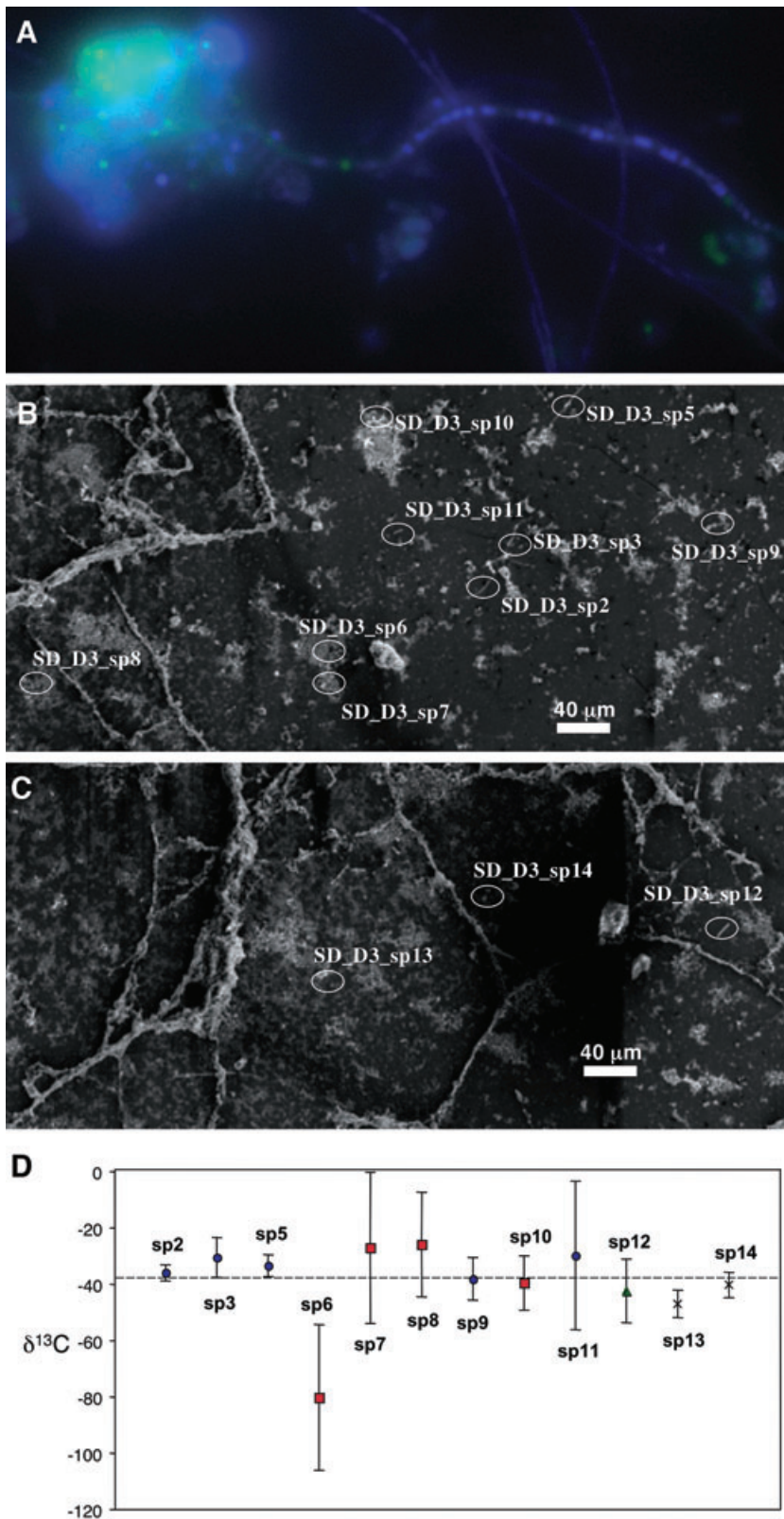
Fig. 4. *In situ* growth of seep microbiota observed and studied on glass slides and silicon wafers from the third hole of 'SD' peeper (sample ID for this silicon wafer is SD_D3).
A. Image shows the results of CARD-FISH (based on Arch915/DAPI). The archaeal probe (green) does not hit the ubiquitous bacterial filaments (stained blue with DAPI) found all over all of the slides and wafers after 14 months in a seep.
B and C. SEM images showing bacterial filaments and biofilms targeted for SIMS $\delta^{13}C$ analysis using the same conditions listed previously with the exception that no charge compensation was used with this conductive surface.
D. The $\delta^{13}C$ compositions of filaments (blue circles), biofilms (red squares), a rod (green triangle) and cocci (black Xs) shown in (B) and (C).

spatial scales may be a unique biogeochemical signature of methane seep microbiota.

Experimental procedures

Samples

Push-cores (PC55 and PC59) were recovered at the Northern Ridge of Eel River Basin methane seeps at a depth of 518 m (N 40 48.6893; W 124 36.6785). The *in situ* growth experiment involved placing two series of seven 1-inch-diameter glass slides and seven 1 inch Si-wafers into a pore-water peeper where the surfaces were in contact with a 1 ml internal volume of sterile anoxic 20 g l^{-1} NaCl solution and behind a polycarbonate filter (Fig. S1). The porewater peeper was inserted in a methane seep microbial mat in the Eel River Basin for 14 months (N 40 48.6922; W 124 36.6785). In one series, the slides and wafers were behind a 0.2 μm polycarbonate filter (Whatman), and in the other series the slides and wafers were behind a 12 μm polycarbonate filter. Following an approximate 2 week equilibration time, the internal peeper cell fluid should have been in chemical equilibrium with the sediment porewater similar to the original application of a peeper by Hesslein (1976). After recovery, the glass slides were carefully fixed (0.2% paraformaldehyde for 1 h) and then rinsed through an ethanol dehydration series (2 min in 50% ethanol : PBS, 2 min in 75% ethanol : PBS and 2 min in 100% ethanol). The silicon wafers were rinsed through an ethanol dehydration series without fixation. Both series were stored at −80°C.

Porewater geochemsitry

Porewater sulfide concentrations were measured using a a colorimetric Cline assay (Cline, 1969) spectrometric determination of duplicated samples precipitated shipboard with excess ZnCl. Specifically, the porewater was added to 0.1 ml of 2.8 M ZnCl$_2$ in a N$_2$-filled serum vial. The supernatant of the ZnCl-fixed samples was treated with excess pH 5 BaCl to precipitate BaSO$_4$ so that the concentration of porewater sulfate could be determined by a spectrometric turbidity measurement at 450 nm on a Beckman DU-530 UV/Vis Spectrophotometer. Dissolved inorganic carbon data were determined by spectrometric turbidity measurements (at 600 nm) of 1.9 ml porewater samples fixed in an N$_2$-filled serum vial with 0.1 ml of 3 M NH$_4$Sr(OH$_2$)$_3$. The δ^{13}C composition of the resultant SrCO$_3$ samples were measured on using a Costech/Thermo-Finnigan Delta Plus XP coupled elemental analyser, continuous flow and isotope ratio mass spectrometer (EA-CF-IRMS). For methane, shipboard, 5 ml sediment plugs were placed in vials with 1 M NaOH. The headspace was then flushed with N$_2$ and the samples stored for later analysis. The δ^{13}C of porewater CH$_4$ was determined by gas chromatography-isotope ratio mass spectrometry (Isotech Laboratories, Champaign, IL, USA).

FISH-SIMS

FISH staining [using EelMSMX_932 and Eub338 (3mix) probes] and mapping of cell targets for SIMS analysis were conducted as previously described (Orphan *et al.*, 2001b). Carbon isotopic compositions of the identified cells were measured using the UCLA CAMECA 1270 ion microprobe. The SIMS was performed on selected cells using a 0.05–0.1 nA, ~15 μm, Cs+ primary ion beam. The δ^{13}C compositions of cells were determined on a Cameca 1270 using a EM-EM multicollector configuration with ^{12}C$_2$-detected with an off-axis electron multiplier and ^{12}C^{13}C$^-$ measured on-axis with the central on-axis detector. Charge compensation was achieved using a normal incident electron gun and a gold coat applied to the sample after FISH microscopy.

Radiotracer rate measurements

Rates of methane oxidation were determined using the ^{14}CH$_4$ tracer method of Joye and colleagues (2004). As with measured rates of AOM, relative rates of sulfate reduction, CO$_2$-reductive methanogenesis and acetoclastic methanogenesis were monitored using radiolabelled substrates (^{35}SO$_4$$^{2-}$, H^{14}CO$_3$$^-$ and ^{14}CH$_3$^{14}COO$^-$), but these have been shown as percentages of injected metabolite consumed rather than a metabolic rate because the indigenous concentrations of these substrates were not known.

CARD-FISH and SEM

The LEO 1430VP variable pressure scanning electron microscope at UCLA was used to image the surface of the several recovered silicon wafers using typical SEM conditions. The wafers and slides from the third position in the peeper were chosen for further study. CARD-FISH based on Arch915 was performed on the glass slide (Pernthaler *et al.*, 2002) to identify the ubiquitous filaments observed visually and with the SEM.

Acknowledgements

References

Barnes, R.O., and Goldberg, E.D. (1976) Methane production and consumption in anoxic marine sediments. *Geology* **4:** 297.

Boetius, A., Ravenschlag, K., Schubert, C.J., Rickert, D., Widdel, F., Gieseke, A., *et al.* (2000) A marine microbial consortium apparently mediating anaerobic oxidation of methane. *Nature* **407:** 623–626.

Cline, J.D. (1969) Specrophotometric determination of hydrogen sulfide in natural waters. *Limnol Oceanogr* **14:** 454–458.

Hallam, S.J., Putnam, N., Preston, C.M., Detter, J.C., Rokhsar, D.S., Richardson, P.M., and DeLong, E.F. (2004) Reverse methanogenesis: testing the hypothesis with environmental genomics. *Science* **305:** 1457–1462.

Hesslein, R.H. (1976) An *in situ* sampler for close interval pore water studies. *Limnol Oceanogr* **21:** 912–914.

Hinrichs, K.U., Hayes, J.M., Sylva, S.P., Brewer, P.G., and DeLong, E.F. (1999) Methane-consuming archaebacteria in marine sediments. *Nature* **398:** 802–805.

Hinrichs, K.U., Summons, R.E., Orphan, V.J., Sylva, S.P., and Hayes, J.M. (2000) Molecular and isotopic analysis of anaerobic methane-oxidizing communities in marine sediments. *Organic Geochem* **31:** 1685.

Hinrichs, K.U., and Boetius, A. (2002) The anaerobic oxidation of methane: new insights in microbial ecology and biogeochemistry. In *Ocean Margin Systems*. Wefer, G., Billett, G., Hebbeln, D., Jørgensen, B.B., Schlüter, M., and Weering, T.V. (eds). Heidelberg: Springer-Verlag, pp. 457–477.

Hoehler, T.M. (1994) Field and laboratory studies of methane oxidation in an anoxic marine sediment: Evidence for a methanogen-sulfate reducer consortium. *Global Biogeochem Cycles* **8:** 451.

House, C.H., Schopf, J.W., McKeegan, K.D., Coath, C.D., Harrison, T.M., and Stetter, K.O. (2000) Carbon isotopic composition of individual Precambrian microfossils. *Geology* **28:** 707–710.

Joye, S.B., Boetius, A., Orcutta, B.N., Montoya, J.P., Schulz, H.N., Erickson, M.J., and Lugo, S.K. (2004) The anaerobic oxidation of methane and sulfate reduction in sediments from Gulf of Mexico cold seeps. *Chemical Geology* **205:** 219–238.

Knittel, K., Lösekann, T., Boetius, A., Kort, R., and Amann, R. (2005) Diversity and distribution of methanotrophic Archaea at cold seeps. *Appl Environ Microbiol* **71:** 467–479.

Krzycki, J.A., Kenealy, W.R., DeNiro, M.J., and Zeikus, J.G. (1987) Stable carbon isotope fractionation by *Methanosarcina barkeri* during methanogenesis from acetate, methanol, or carbon dioxide-hydrogen. *Appl Environ Microbiol* **53:** 2597–2599.

Kvenvolden, K.A., and Field, M.E. (1981) Thermogenic hydrocarbons in unconsolidated sediment of Eel River basin, offshore northern California. *AAPG Bull* **65:** 1642–1646.

Leloup, J., Loy, A., Knab, N.J., Borowski, C., Wagner, M., and Jørgensen, B.B. (2007) Diversity and abundance of sulfate-reducing microorganisms in the sulfate and methane zones of a marine sediment, Black Sea. *Environ Microbiol* **9:** 131–142.

Michaelis, W., Seifert, R., Nauhaus, K., Treude, T., Thiel, V., Blumenberg, M., *et al.* (2002) Microbial reefs in the Black Sea fueled by anaerobic oxidation of methane. *Science* **297:** 1013–1015.

Moran, J.J. (2008) Methyl sulfides as intermediates in the anaerobic oxidation of methane. *Environ Microbiol* **10:** 162.

Nauhaus, K., Boetius, A., Kruger, M., and Widdel, F. (2002) In vitro demonstration of anaerobic oxidation of methane coupled to sulphate reduction in sediment from a marine gas hydrate area. *Environ Microbiol* **4:** 296–305.

Niemann, H., Losekann, T., de Beer, D., Elvert, M., Nadalig, T., Knittel, K., *et al.* (2006) Novel microbial communities of the Haakon Mosby mud volcano and their role as a methane sink. *Nature* **443:** 854–858.

Orcutt, B., Boetius, A., Elvert, M., Samarkin, V., and Joye, S.B. (2005) Molecular biogeochemistry of sulfate reduction, methanogenesis and the anaerobic oxidation of methane at Gulf of Mexico cold seeps. *Geochim Cosmochim Acta* **69:** 4267–4281.

Orphan, V.J., Hinrichs, K.U., Ussler, W., Paull, C.K., Taylor, L.T., Sylva, S.P., *et al.* (2001a) Comparative analysis of methane-oxidizing archaea and sulfate- reducing bacteria in anoxic marine sediments. *Appl Environ Microbiol* **67:** 1922–1934.

Orphan, V.J., House, C.H., Hinrichs, K.U., McKeegan, K.D., and DeLong, E.F. (2001b) Methane-consuming archaea revealed by directly coupled isotopic and phylogenetic analysis. *Science* **293:** 484–487.

Orphan, V.J., House, C.H., Hinrichs, K.U., McKeegan, K.D., and DeLong, E.F. (2002) Multiple archaeal groups mediate methane oxidation in anoxic cold seep sediments. *Proc Natl Acad Sci U S A* **99:** 7663–7668.

Orphan, V.J., House, C.H., and Goffredi, S.K. (2008) Archaea, methane and oases of the deep. In *Life Strategies of Microorganisms in the Environment and in Host Organisms.* Amann, R., Goebel, W., Reinhold-Hurek, B., Schink, B., and Widdel, F. (eds), pp. 19–23.

Orphan, V.J., Ussler, III, B., Naehr, T.H., House, C.H., Hinrichs, K.U., and Paull, C.K. (2004) Geological, geochemical, and microbiological heterogeneity of the seafloor around methane vents in the Eel River Basin, offshore California. *Chemical Geology* **205:** 265–289.

Pancost, R.D., Sinninghe Damste, J.S., de Lint, S., van der Maarel, M.J.E.C., Gottschal, J.C., and the Medinaut Shipboard Scientific Party. (2000) Biomarker evidence for widespread anaerobic methane oxidation in Mediterranean sediments by a consortium of methanogenic archaea and bacteria. *Appl Environ Microbiol* **66:** 1126–1132.

Pernthaler, A., Pernthaler, J., and Amann, R. (2002) Fluorescence *in situ* hybridization and catalysed reporter deposition for the identification of marine bacteria. *Appl Environ Microbiol* **69:** 3094–3101.

Pernthaler, A., Dekas, A.E., Brown, C.T., Goffredi, S.K., Embaye, T., and Orphan, V.J. (2008) Diverse syntrophic partnerships from deep-sea methane vents revealed by direct cell capture and metagenomics. *Proc Natl Acad Sci* **105:** 7052–7057.

Reeburgh, W.S. (1976) Methane consumption in Cariaco Trench waters and sediments. *Earth Planet Sci Lett* **28:** 337.

Reeburgh, W.S. (1996) 'Soft Spots' in the global methane budget. In *Microbial Growth on C1 Compounds*. Lidstrom, M.E., and Tabita, F.R (eds). Boston, MA, USA: Kluwer Academic Publishers, pp. 334–342.

Teske, A., Hinrichs, K.U., Edgcomb, V., de Vera Gomez, A.,

Kysela, D., Sylva, S.P., *et al.* (2002) Microbial diversity of hydrothermal sediments in the guaymas basin: evidence for anaerobic methanotrophic communities. *Appl Environ Microbiol* **68:** 1994–2007.

Valentine, D.L. (2002) Biogeochemistry and microbial ecology of methane oxidation in anoxic environments: a review. *Antonie Van Leeuwenhoek* **81:** 271–282.

Wegener, G., Niemann, H., Elvert, M., Hinrichs, K.U., and Boetius, A. (2008) Assimilation of methane and inorganic carbon by microbial communities mediating the anaerobic oxidation of methane. *Environ Microbiol* **10:** 2287–2298.

Supporting information

Additional Supporting Information may be found in the online version of this article:

Fig. S1. An drawing of the *in situ* incubation device ('pore-water peeper') used to place Si-wafers and glass slides into seep sediment. There are a series of seven 1-inch-diameter glass slides and seven 1 inch Si-wafers placed so that the surfaces were in contact with a 1 ml internal volume of anoxic 20 g l^{-1} NaCl solution. The slides and wafers are behind either a 0.2 μm polycarbonate filter (Whatman) or a 12 μm polycarbonate filter. There is also a mesh covering protecting the filters. Insert: photograph of peeper after 14 months in seep sediment. The mesh covering can be seen in each of the holes.

Table S1. FISH-SIMS δ^{13}C data for microorganisms in PC55 from the Eel River Basin.

Please note: Wiley-Blackwell are not responsible for the content or functionality of any supporting materials supplied by the authors. Any queries (other than missing material) should be directed to the corresponding author for the article.